Influence of Vegetation Structure on Urban Microclimate: A computational study on UHI mitigation using OpenFOAM

Chinmay Rothe[1], Patrick Kastner[2] and Marionyt Tyrone Marshall[3]

[1,2] Georgia Institute of Technology, Atlanta, GA, USA

[3] AIA, NOMA, Assoc. ASHRAE, LEED AP BD+C

Senior Research Lead in Regenerative Design, Senior Associate, Perkins+Will

E-mail: crothe3@gatech.edu

Abstract

The importance of vegetation in mitigating the urban heat island effect by cooling the urban microclimate cannot be overstated, especially given the rapid urbanization that impacts it. Urban microclimate parameters, such as temperature and humidity changes in the atmosphere, further influence the adverse effects on outdoor thermal comfort.

This study examines vegetation's cooling potential by evaluating different characteristics, such as stomatal resistance, moisture content, leaf temperature, and heat transfer coefficients, among different tree sizes. The primary objective is to simulate an urban scenario using *urbanmicroclimateFOAM*, incorporating detailed characteristics of a single vegetation species, Acer rubrum (red maple), and an urban block model over multiple hours daily. Using an EPW file enables accurate input of local climate data to optimize results.

The findings highlight the importance of tree size, stomatal resistance, LAD value, and wind speed in affecting the moisture content and temperature of the surrounding environment, further affecting the cooling potential and thermal comfort. Moreover, the effect of different-sized red maple trees on surrounding temperature and their location can considerably alter temperature and moisture content. Furthermore, vegetation and climate parameters influence heat transfer and evapotranspiration, highlighting their role in urban cooling.

Future research should expand on this work by examining different species and soil characteristics for a more comprehensive understanding of the cooling potential through vegetation in the urban microclimate.

Keywords: Urban microclimate, Vegetation, Stomatal Resistance, LAD, Moisture content, Relative humidity, Air temperature

1. Introduction

Urbanization worldwide has contributed to pressing environmental issues [1], such as elevated temperatures, reduced wind speed, and low-quality outdoor thermal comfort. [2]. Additionally, frequent, intense, and prolonged heat waves affect the urban areas. [3]. Studies have shown that urban areas magnify heat waves due to building materials as opposed to vegetated rural areas [4]. As suggested by the Author [5], global warming is not the only contributor to the urban heat island effect; instead, replacing vegetation and anthropogenic emissions are some of the leading causes. In addition, shading of a tree plays an important role in mitigating surface temperatures by absorbing and reflecting intense solar radiation, reducing its reach to ground and building surfaces [6]. Thus, increasing the amount of vegetation on an urban scale has the potential to abate daytime UHI., At the same time, it identified that vegetation can also reduce high temperatures by decreasing radiant exchange and evaporative cooling [7], [4].

The higher Lad consideration exhibited higher transpiration rates studied of six different species used as street trees,

reducing microclimate temperature [8]. The temperature reduction occurs with a reduction in stomatal resistance [9]. Consequently, a higher stomatal resistance increases the leaf temperature, resulting in a lower cooling potential. This cooling potential is also influenced by the absorbed radiative heat into sensible and latent heat fluxes [10]. There has been extensive study on the cooling potential of urban vegetation, yet the influence of red maple (*Acer rubrum*) on microclimate cooling still needs to be explored.

In another study by [11] highlighted considerable differences in how much water red maple transpire depending on their management conditions. This finding highlights the crucial ways these trees respond to the environment. A recent study [12] demonstrates the impressive ability of red maple to thrive in urban environments, highlighting physiological acclimation in larger urban areas. There's a notable gap in using advanced tools like Computational Fluid Dynamics, such as OpenFOAM, to study the cooling potential of red maple trees. This creates an important opportunity for the research to explore urban vegetation planning and its effect on local temperatures.

2. Overview

2.1 Mitigation strategies for the urban heat island effect

Urbanization has impacted significant modifications in habitation patterns, which led to the consolidation of population and economic activities, further influencing the rise in adverse environmental effects, such as Co2 emissions [13]. This urban concentration has led to the UHI effect, often characterized by higher urban temperatures than adjacent rural areas [14]. The complex interactions between net positive thermal balance and global warming have intensified urban overheating, affecting the urban climate [15].

Furthermore, the UHI effect hurts the comfort and health of humans [16]. There are also many progressive implementations by city planners of various sustainable solutions to alleviate the effect of UHI and incorporate climate change. The thermal stress in an urban environment is mitigated through a few strategies, such as urban green spaces, cool roofs, city gardens, green infrastructure, and tree canopies [13]. Urban greening is crucial in promoting cooling for the local environment. Along with other green infrastructure, parkland has been considered an influential strategy for containing urban heat. The study uses greenery to alleviate the UHI effect [17].

2.2 Vegetation-based cooling strategies for UHI mitigation

The vegetation is instrumental in abating the UHI effect due to a reduction in temperature along with an improved urban microclimate. Trees in urban environments have a significant cooling effect, lowering daily average temperatures by 3°C, whereas maximum temperatures by 5.23°C [18]. Studies have also found that 10% growth in vegetation cover further fosters reduced UHI intensity, leading to thermal comfort and a steady urban environment [19]. The microclimate also affects the cooling ability of urban vegetation; specifically, intense rainfall and irrigation improve the grassland's cooling effect in hot-dry conditions, while high humidity restricts cooling efficiency. Moreover, intense wind speeds help evaporative cooling and airflow by improving tree-covered vegetation's performance, especially in Mediterranean urban climates [20].

Furthermore, combining different strategies with vegetation can really amplify their effectiveness. The "cool city" model used in tropical areas integrates cool pavements, green roofs, and more plants to reduce UHI effects. Resulting in comfortable urban areas. Additionally, vegetation in this model contributes to cooling more than other elements by considerably affecting the surface energy balance [21]. Regarding infrastructure design, green and blue space systems collectively fight the UHI effect and improve urban microclimate resilience. These systems provide a holistic approach to UHI mitigation by reducing heat stress in boundary-level conditions and enhancing cooling through the canopy layer [22]. The efficacy of vegetation is affected by its physiological attributes. Tree size is directly related to the cooling benefits of transpiration due to the heat extraction ability from the surrounding environment. Lager trees provide broad shading, improving thermal comfort compared to smaller rows of trees [10].

2.3 Impact of vegetation characteristics on microclimate

Vegetation cover and height considerably impact the soil temperatures, especially in tundra ecosystems. The study demonstrated that tall vegetation and proliferated shrub cover in western grassland showcase cooler soil temperatures during the growing season. Moreover, soil temperatures can increase by 0.24°C due to a 10% increase in shrub cover, while vegetation growth of 1cm can reduce temperature by 0.17°C [23]. The selection and location of the correct tree are crucial. Tree species and their placement should account for available space, a climate that can maximize cooling potential, and growth needs [24].

Furthermore, Tree species and canopy structures showcase crucial microclimate patterns in forest ecosystems. Furthermore, southeast Missouri, northern Wisconsin, and the Pacific Northwest show increased shortwave radiation in daytime disturbed forest patches [25]. Another study in Guangzhou, China, underscores the importance of different evergreen species of diverse nature in their cooling potential of air, rising relative humidity, and lowering solar radiation. It highlights the tree species' substantial effect on the microclimate regulations. The summer readings show how

trees increase relative humidity by 3-11% and lower solar radiation below the canopies by 85-95% [26]. These cooling potentials specifically impact extreme weather, such as droughts, which reduces the microclimatic cooling potential [27].

To combat the UHI effect, tree canopy density size along with ground surface cover are essential. Urban parks that have abundant greenery cool their surroundings, reducing the UHI effect [28]. Furthermore, tree cover and plants also cool temperature in the daytime and provide better thermal comfort at night, especially in tropical cities [29]. Additionally, tree types, planting arrangements, and scattered green patches quantify the efficacy of cooling. The larger and simpler patches result in individual patch cooling, while complex arrangements cool areas at a broader scale [30,31]. The vegetation results in overall solar radiation absorption, further reducing the air temperature and increasing evapotranspiration. This process further influences building energy usage for lighting, cooling, and heating [4,32].

2.4 CFD Modeling for urban microclimate

CFD has evolved as an immensely proficient and adaptable tool for urban microclimate analysis, offering essential insights into intricate communication within complex urban settings [33]. CFD simulations are beneficial for studying heat and mass transfer processes, especially when restricted by urban obstacles such as buildings, and they enable in-depth insights into microclimatic conditions [34]. Regardless of the benefits of economic efficiency and flexibility related to physical modeling, technical intricacies keep CFD underutilized in the early stages of urban planning [35]. Advanced CFD models developed using OpenFOAM, such as urbanMicroclimateFoam, demonstrate the CFD potential of urban microclimate studies. The models simulate heat and moisture transfer in air and porous materials, turbulent wind flow, and radiation exchange, offering a detailed analysis system for urban settings [3]. The relationship between vegetation and its environment is fundamentally multi-physical and marked by heat, momentum, mass with air, and radiative exchange. The efficacy in the model for this relationship is done through a porous medium, which allows for a valid approximation of the thermal effect of vegetation [36–38].

Furthermore, this method is useful for understanding the use of vegetation in urban environments, especially the cooling potential influence and its impact on enhancing thermal comfort [39,40]. Similar techniques have been widely used to analyze the impact of vegetation on the microclimate. CFD utilization simulating vegetation can reveal the relationship between urban heat fluxes and airflow to alleviate the UHI effect [41,42]. The experimental study corresponds to CFD methods by offering real-life data; however, it needs more clarity in illustrating the inherent regulatory mechanisms. Additionally, a comprehensive analysis that offers in-depth insights into the influence of vegetation on outdoor microclimate can be achieved by incorporating CFD simulations with theoretical analyses [9].

3. Methodology

3.1 Study area and data collection

The study simulates an urban street canyon environment in Atlanta, Georgia, which provides a lively yet restricted urban area ideal for investigating local climate changes. Atlanta's urban area offers a conventional urban morphology distinguished by dense settlements, street canyons, and sprawling vegetation. Credible sources, such as relevant research papers, verified online government databases, and the OpenFOAM modeling wiki, are used to acquire information on vegetation parameters, meteorological conditions, and urban morphology. Additionally, essential physical vegetation parameters were minimum stomatal resistance, Leaf Area Density (LAD), leaf length, and tree height. These parameters provide the groundwork for the vegetation modeling simulation inputs.

3.2 CFD Model Setup

The CFD simulation scenarios were modeled in Rhino and implemented using the grasshopper plugin urbanMicroclimate solver, an OpenFOAM-based tool. The site-specific approach adopted in this study ensures the important spatial resolution required to register the influence of vegetation on a community scale. The multi-region formulation of OpenFOAM handles density differences across various subdomains.

The CFD model is combined with the Heat, Air, and Moisture (HAM) model to account for the dynamic moisture and heat storage in porous urban materials like street pavement and walls [3]. The computational domain contains two isolated building structures represented as 'Brep' geometries inside the grasshopper and several trees as meshes surrounding the building. The simulation scenarios included variations in the tree heights (3m, 7m, and 14m). The computational domain represents a 25-m-wide street canyon, 12-m high x 13-m wide buildings, and consistent tree types throughout each scenario. The Computational Wind Engineering (CWE) best practice guidelines are followed to ensure an appropriately sized domain for accurate solutions [43].

3.3 Vegetation modeling

As described in [10], trees are modeled as porous mediums with sink and source terms for momentum, moisture, and heat. Tree foliage generates latent and sensible heat fluxes and long ``wave heat exchange, shading, and aerodynamic effects of the

tree. A constant moisture availability is assumed for roots in the soil, ensuring that stomata remain open and functional under all conditions. Discretized tree foliage in finite volume, along with LAD, quantifies the distribution of leaves in a volume [44]. A leaf energy model simulates the heat exchange between tree canopy and air, excluding dynamic heat storage in leaves [45].

The study involves three iterations:

- Iteration 1: Trees with a height of 3m. *(Figure 1)*
- Iteration 2: Trees with a height of 7m. *(Figure 2)*
- Iteration 3: Trees with a height of 14m. *(Figure 3)*

Each iteration differs in input parameters such as LAD values, minimum stomatal resistance, leaf length, and tree height. The duration of the simulation performance is mid-June, from 11 a.m. to 4 p.m. (5 hours). Additionally, a comparative analysis is conducted with just one tree of 7 m height in the iteration 2 setting, named Iteration 2b, during mid-March from 11 a.m. to 7 p.m. (9 hours). However, the tree count remains constant across all iterations except for the scenario with a single tree.

Wind speed variations were also considered in other iterations using a design of experiments approach to generate different parameter combinations. Evapotranspiration helps evaluate the cooling potential of vegetation in the model, which is crucial for UHI mitigation. The tree's evapotranspiration, shading, and sheltering enable temperature reduction. The Multiscale approach modeling the heat and moisture balance at the leaf level results in evaporative cooling, stomatal behavior, and shading. This integration helps to analyze the comprehensive influence of vegetation on urban microclimate [46].

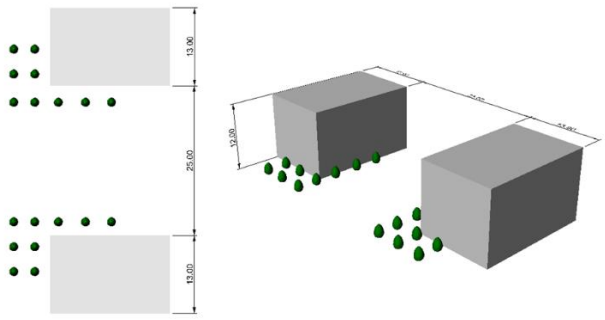

Figure 3.1.1: Iteration 1 has tree height of 3 m, building of 12 m high x 13 m wide, and 25 m wide street in between.

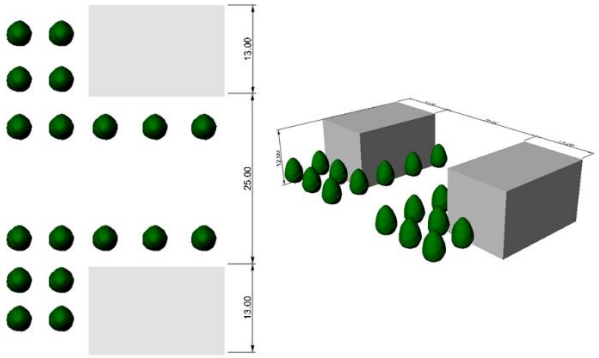

Figure3.2.2: Iteration 1 has tree height of 14 m, building of 12 m high x 13 m wide, and 25 m wide street in between.

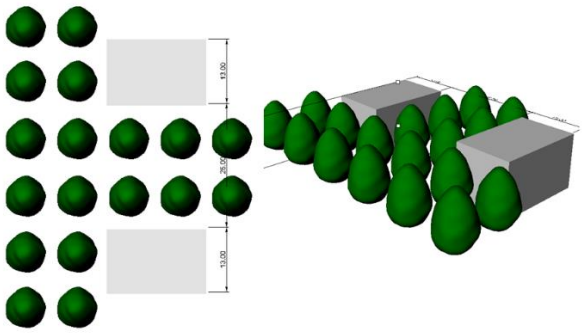

Figure.3.3.3: Iteration 1 has tree height of 14 m, building of 12 m high x 13 m wide, and 25 m wide street in between.

4. Results and findings

4.1 Iteration 1

In iteration 1 (Figure 3.3.1), vegetation parameters include a tree height of 3 m, LAD 1 m^2m^3, leaf length of 0.1 m, and minimum stomatal resistance (rs_{min}) of 150 sm^2, with a wind speed set at 7 m/s. The simulation is performed in mid-June, between 11 a.m. and 4 p.m., using the Atlanta-Hartsfield-Jackson International Airport EPW weather file from 2007–2021. According to Graph 4.1.1, the average temperature increases from 302.2 K at 11 a.m. (x-axis: 3600 seconds) to 301.6 K at 4 p.m. (x-axis: 18000 seconds), highlighting the temperature rise of 1.4 K.

The minimum temperature (min T) was recorded at 299.5 K, while the maximum temperature reached 309.0 K, as observed at only specific sensor points. Inside the study area around the vegetation, the predominant maximum temperature (max T) is 302.5 K. When correlating temperature patterns with wind velocity, areas experiencing the most significant temperature rise between 11 a.m. and 4 p.m. coincide with zones of low wind speed. The relationship between stomatal resistance and leaf temperature is intricate.

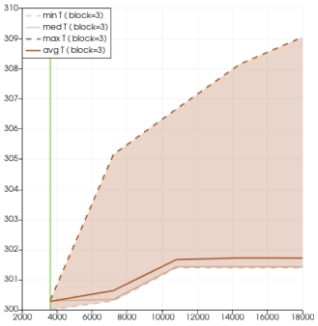

Graph 4.1.1: Air temperature (11 a.m. to 4 p.m.)

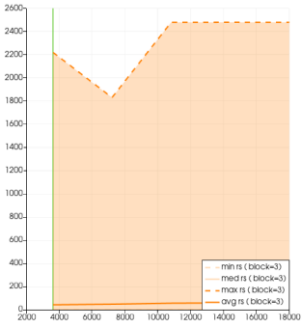

Graph 4.1.2: stomatal resistance (11 a.m. to 4 p.m.)

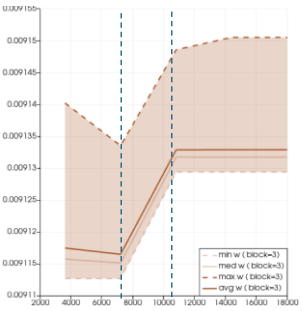

Graph 4.1.3: Moisture content (11 a.m. to 4 p.m.)

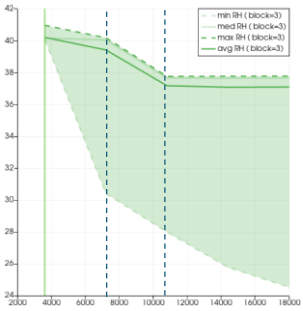

Graph 4.1.4: Relative humidity (11 a.m. to 4 p.m.)

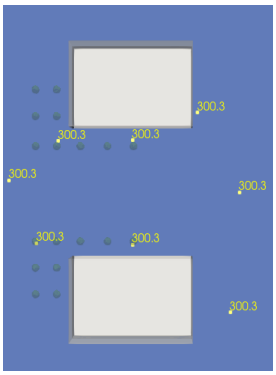

Figure 4.1.1: Air temperature: 11 a.m. to noon

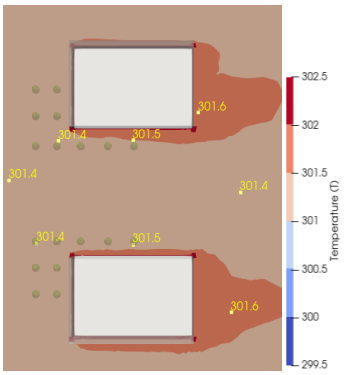

Figure 4.1.2: Air temperature from 3 p.m. to 4 p.m.

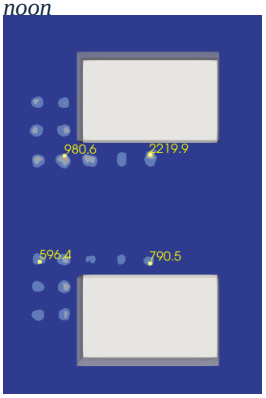

Figure 4.1.3: Stomatal resistance:11 a.m. to 12 noon.

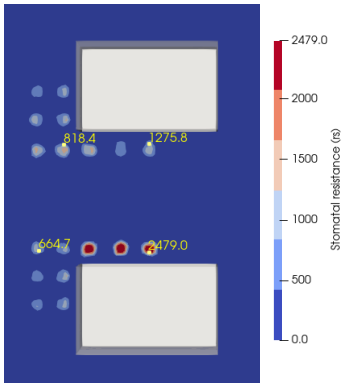

Figure 4.1.4: Stomatal resistance from 3 p.m. to 4 p.m.

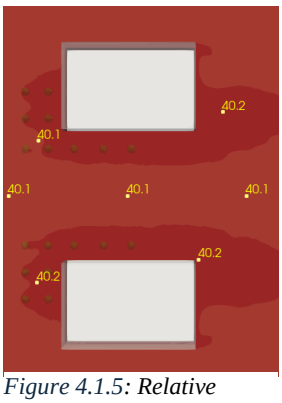

Figure 4.1.5: Relative humidity from 11 a.m. to 12 noon.

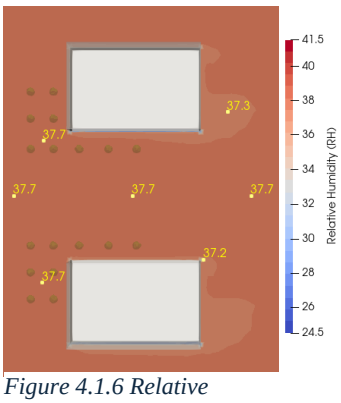

Figure 4.1.6 Relative humidity from 3 p.m. to 4 p.m.

Furthermore, an increase in leaf temperatures can cause more resistance in the stomata (Figures 4.1.3 and 4.1.4), but this pattern is inconsistent across all conditions. This variation depends on external factors such as the timing of observations. Simulations from 11 a.m. to 4 p.m. in June show higher temperatures, especially between 3 to 4 p.m., influencing the observed variations.

Additionally, as per (Graphs 4.1.3 and 4.1.4), observations reveal an inverse relationship between moisture content and relative humidity (RH). Increasing moisture content aligns with decreasing RH (Figure 4.1.5 and 4.1.6), as warmer air holds more water vapor, resulting in lower RH than cooler air with the same moisture level [47]. Graphs 4.1.3 and 4.1.4 illustrate this trend between 12 p.m. and 1 p.m. (time: x-axis: 7500–11,000 seconds), where a rise in moisture content coincides with a decline in RH, reflecting an overall increase in air temperature.

4.1.1 Iteration 1 analysis.

We can examine various relationship inputs by superimposing the analysis plane on the z and y axes. Specifically, we can explore how rising afternoon temperatures negatively affect cooling potential. Thus, we can determine how vegetation parameters of iteration affect the microclimate

4.2 Iteration 2

Iteration 2 (Figure 3.3.2) has a mid-size tree height of 7 m, LAD 1.5 m^2m^3, a leaf length of 0.15 m, minimum stomatal resistance (rs_{min}) of 275 sm^2, and wind speed of 7 m/s for mid-June from 11 a.m. to 4 p.m. The weather file is the Atlanta-Hartsfield-Jackson International Airport EPW from 2007–2021. According to Graph 4.2.1, the temperature change from 11 a.m. (x-axis: 3600) to 4 p.m. (x-axis:18000) for Average temperature (T) is 300.1 k to 301.5 k, a 1.4 k rise, while min T is 300.1 and max T is 308.2 recorded for a couple of sensors as reflected in the graph. However, the area for the study surrounding the vegetation shows a predominantly Max T of

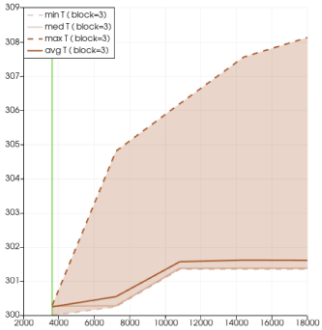

Graph.4.2.1: Air temperature (11 a.m. to 4 p.m.)

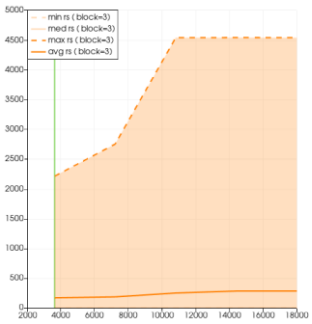

.Graph 4.2.2: Stomatal Resistance (11 a.m. to 4 p.m.)

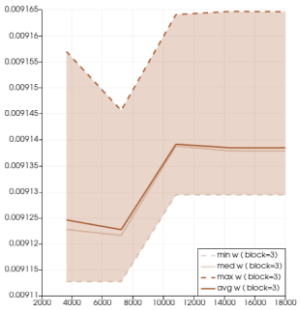

Graph 4.2.3: Moisture content (11 a.m. to 4 p.m.)

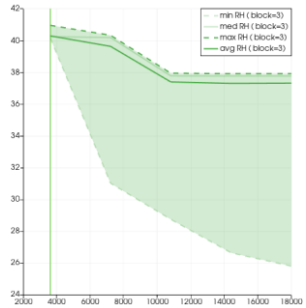

Graph 4.2.4.: Relative humidity (11 a.m. to 4 p.m.)

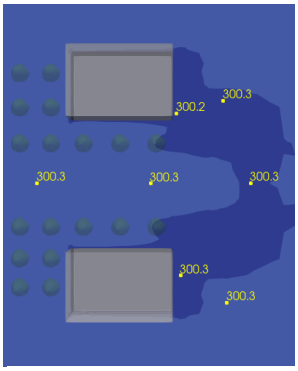

Figure 4.2.1 Air temperature bfrom 11 a.m. to 12 noon

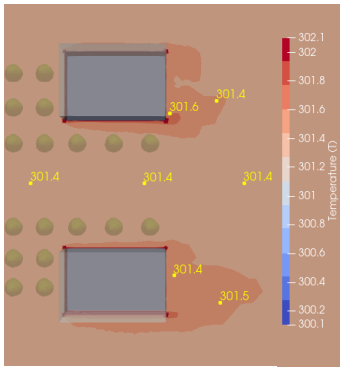

Figure 4.2.2: Air temperature from 3 p.m. to 4 p.m.

302.1 k. When we compare the temperature pattern in the domain with wind velocity, we can see the most significant difference in the rise of temperature from 11 a.m. to 4 p.m., near areas with low wind speed, the same as iteration 1.

Furthermore, a consistent pattern of stomatal resistance and leaf temperature is followed in this iteration, too. However, in iteration 2, the tree height and analysis plane are at a higher level, positioned at crown center heights, resulting in the relationship between rising stomatal resistance (Figures 4.2.3 and 4.2.4) and leaf temperature values with the previous iteration despite different tree heights. The increase in leaf temperature by approximately 1-2°C coincides with the increasing air temperature. Graph 4.2.3 showcases a sharp rise in stomatal resistance at noon (x-axis: 7500 seconds) due to

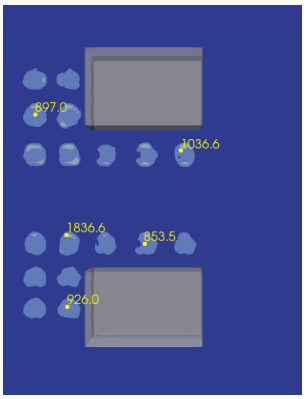

Figure 4.2.3: Stomatal resistance from 11 a.m. to noon

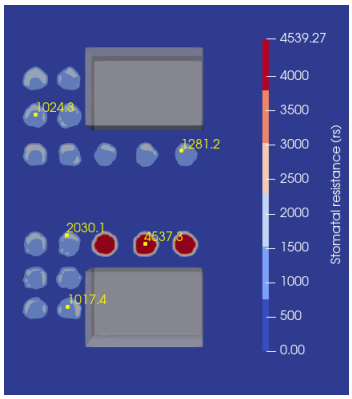

Figure 4.2.4: Stomatal resistance from 3 p.m. to 4 p.m.

increasing temperature in mid-June, which further affects the cooling potential of the vegetation.

During these 5-hour (11 a.m. to 4 p.m.), the atmosphere's moisture content rises in areas with lower stomatal resistance and spreads over larger areas. This indicates that tree size (≥7 m), larger leaves, and higher LAD values contribute to the rising moisture content.

Moreover, (Graph 4.2.4, Figure 4.2.5, and Figure 4.2.6) showcase relative humidity patterns, which are decreasing with rising moisture content. The areas with high moisture content are larger in iteration 2 than in iteration 1 due to increased tree sizes. This iteration, with mid-sized trees and higher LAD values, showcases fewer changes in relative humidity. Graph 4.2.4 displays that the reduction in RH values is comparatively less drastic than in iteration 1, implying that

Figure 4.2.5: Relative humidity from11 a.m. to noon

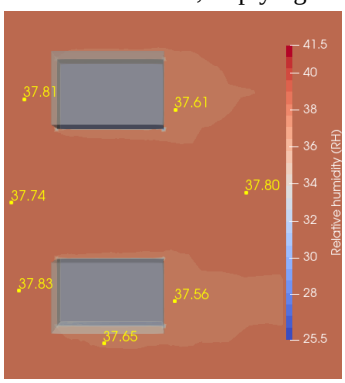

Figure 4.2.6: Relative humidity from 3 p.m. to 4 p.m.

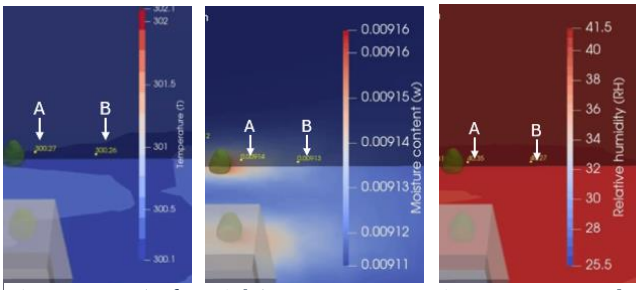

Figure 4.2.7: (Left to right) Temperature, Moisture content, and RH from 11 a.m. to 4 p.m.

increasing air temperatures may be reduced near vegetation-shadowed areas.

4.2.1 Iteration 2 analysis. Figure 4.2.7 displays how tree size significantly affects relative humidity and temperature differences, with better RH values observed near vegetation than further points on the same plane. Analyses of Mark 'A' and 'B' confirm this trend.

4.3 Iteration 3

Iteration 3 (Figure 3.3.3) has a large-size tree height of 14 m, LAD 1-(rs_{min}) of 150 sm^2, and wind speed of 7 m/s for mid-June from 11 a.m. to 4 p.m. The weather file is the Atlanta-Hartsfield-Jackson International Airport EPW weather file from 2007–2021. According to (Graph 4.3.1) the temperature change from 11 a.m. (x-axis: 3600) to 4 p.m. (x-axis:18000) for Average temperature (T) is 300.2k to 301.5 k, a 1.3 k rise,

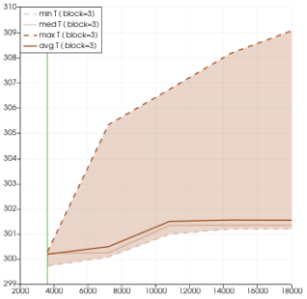

Graph 4.3.1: Air temperature (11 a.m. to 4 p.m.)

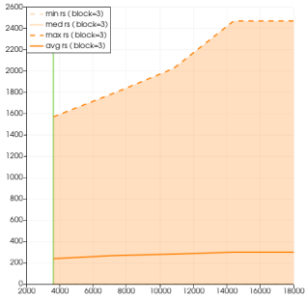

Graph 4.3.2: Stomatal resistance (11 a.m. to 4 p.m.)

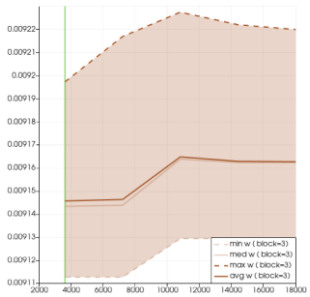

Graph 4.3.3: Moisture content (11 a.m. to 4 p.m.)

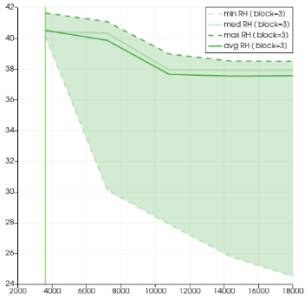

Graph 4.3.4: Relative humidity (11 a.m. to 4 p.m.)

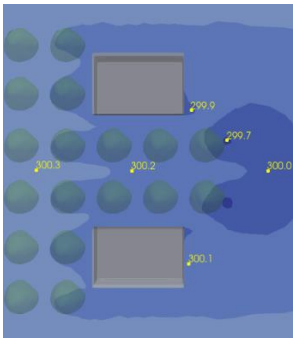

Figure 4.3.1: Air temperature from 11 a.m. to noon

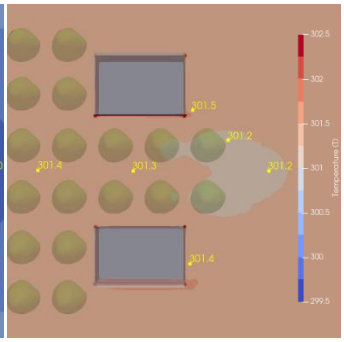

Figure 4.3.2: Air temperature from 3 p.m. to 4 p.m.

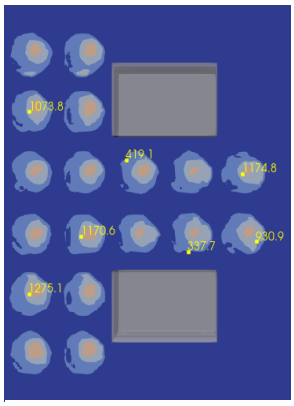

Figure 4.3.3: Stomatal resistance from 11 a.m. to noon

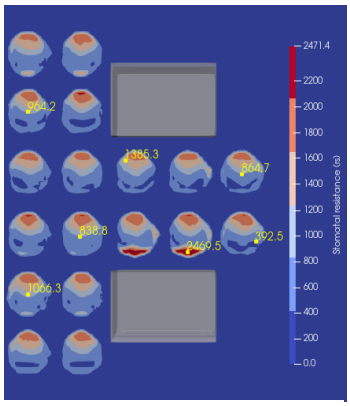

Figure 4.3.4: Stomatal resistance from 3 p.m. to 4 p.m.

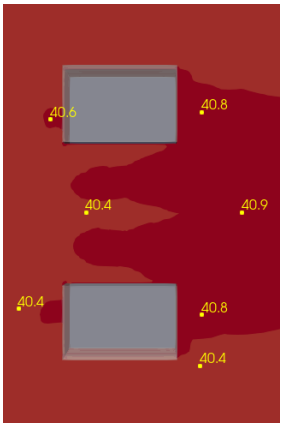

Figure 4.3.5: Relative humidity from 11 a.m. to noon

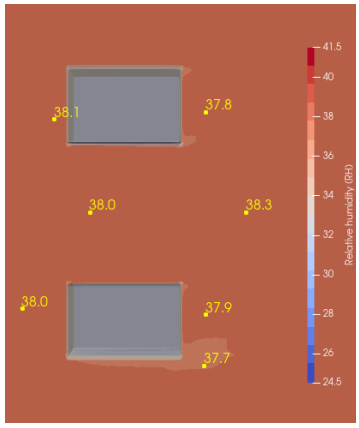

Figure 4.3.6: Relative humidity from 3 p.m. to 4 p.m.

while min T is 299.5 k and max T is 309.0k recorded for a `couple of sensors as reflected in the graph. However, the area for the study surrounding the vegetation shows a predominantly Max T of 302.5k. When we compare the temperature pattern in the domain with wind velocity, we can see a similar rise in temperature from 11 a.m. to 4 p.m. near areas with low wind speed as in the earlier two iterations. Furthermore, with a tree height of 14 m and an analysis plane at 12 m, the crown center across all three sizes should show a similar pattern. Minimum stomatal resistance input (150 sm^2) leads to resistance values up to 2471 sm^2. By comparison, Iteration 2's minimum input (275 sm^2) results in 4539 sm^2, almost double. Tree size affects moisture content; however, stomatal resistance values remain unaffected. Interestingly, while this iteration has bigger leaves than iteration 1, the LAD remains the same as iteration 1.

Additionally, the moisture content pattern is consistent with previous iterations, with increased moisture indicating reduced stomatal resistance and vice versa. Larger trees significantly impact RH (Figures 4.3.5 and 4.3.6) and moisture content ratios. Graphs 4.3.3 and 4.3.4 show

stabilizing relative humidity levels compared to moisture content, with wider ranges observed for larger trees, LAD values, and leaf length.

4.3.1 Iteration 3 analysis. Larger trees enhance relative humidity and moisture content, even during peak mid-June afternoon hours. Lower minimum stomatal resistance and higher LAD values contribute to improved vegetation cooling potential. Observations reveal higher humidity levels under the tree crown.

4.4 Iteration 2b

Iteration 2b has a mid-size tree height of 7 m (only one tree considered for this iteration), LAD 1.5 m^2m^3, a leaf length of 0.15 m, minimum stomatal resistance (rs_{min}) of 275 sm2, a wind speed of 7 m/s for mid-June from 11 a.m. to 4 p.m. The weather file is the Atlanta-Hartsfield-Jackson International Airport EPW weather file from 2007–2021.

Graph 4.4.1 displays the temperature change from 11 a.m. (x-axis: 3600) to 4 p.m. (x-axis: 18000) for the Average temperature (T), which is 300.25 k to 301.40 k, a 1.15 k rise, the min T is 300.25 k, and the max T is 300.45 k recorded for the study surrounding the vegetation. When we compare the temperature pattern in the domain with wind velocity, we can see how having no tree does not slow down the wind compared to earlier iterations.

Furthermore, Iteration 2b features a single tree and showcases the influence of vegetation on relative humidity and moisture content. In this iteration, we keep the same settings as iteration 2 but include only one tree in the domain box. This iteration demonstrates the significance of vegetation presence and its importance in cooling potential, as air temperature, moisture content, and relative humidity remain unchanged or increase in open areas without trees (Figure 4.4.2). The results reinforced the importance of vegetation density and configuration in enhancing microclimatic cooling potential.

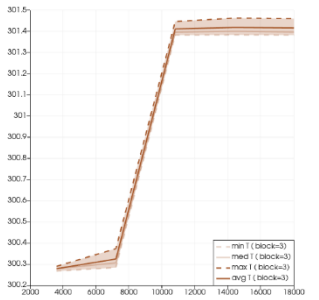

Graph 4.4.1: Air temperature from 11 a.m. to 4 p.m.

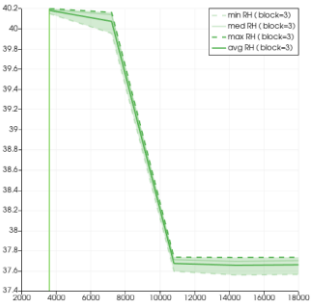

Graph 4.4.2: Relative humidity from 11 a.m. to 4 p.m.

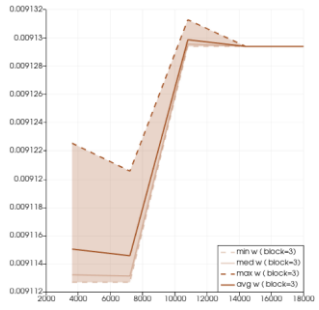

Graph 4.4.3: Moisture content from 11 a.m. to 4 p.m.

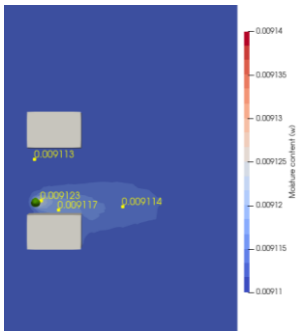

Figure 4.4.1: Moisture content from 11 a.m. to noon

4.5 Iteration 2c

Iteration 2c is for mid-March from 11 am to 7 pm and has a mid-size tree height of 7 m, LAD 1.5 m^2m^3, leaf length of 0.15 m, minimum stomatal resistance (rs_{min}) of 275 sm^2, wind speed of 7 m/s. The weather file is the Atlanta-Hartsfield-Jackson International Airport EPW weather file from 2007–2021. According to Graph 4.5.1, the temperature change from 11 a.m. (x-axis: 3600) to 4 p.m. (x-axis:18000) for Average temperature (T) is 300.2 k to 302.0 k, a 1.8 k rise; however, it drops to 299 k by 7 p.m. (x-axis:32400). The min T is 300.0 k, and the max T is 311.0 k recorded for a couple of sensors,

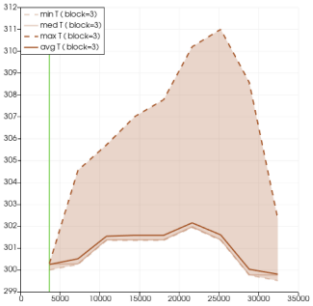

Graph 4.5.1: Air temperature (11 a.m. to 8 p.m.)

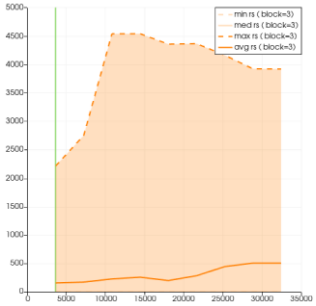

Graph 4.5.2: Stomatal resistance (11 a.m. to 8 p.m.)

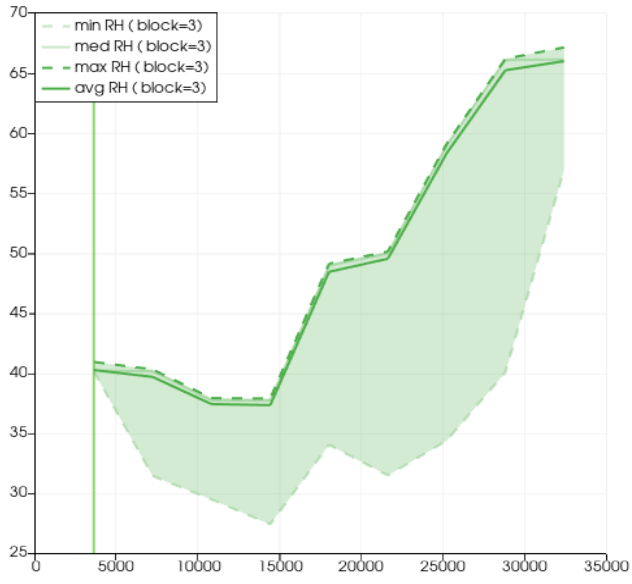

Graph 4.5.3: Relative humidity (11 a.m. to 8 p.m.)

as reflected in the graph. However, the area for the study surrounding the vegetation shows predominantly Max T of 302.k. When we compare the temperature pattern in the domain with other iterations, we can see the temperature rise from 11 a.m. to 4 p.m.; however, the temperature drops again later in the day.

Furthermore, the extra hours after 4 p.m. in March have proven to be much better for increased relative humidity (Graph 4.5.3), moisture content, and lower temperatures. Although March has relatively lower temperatures than June, it indicates a heat threshold, which causes air temperature to drop, enhancing the cooling potential.

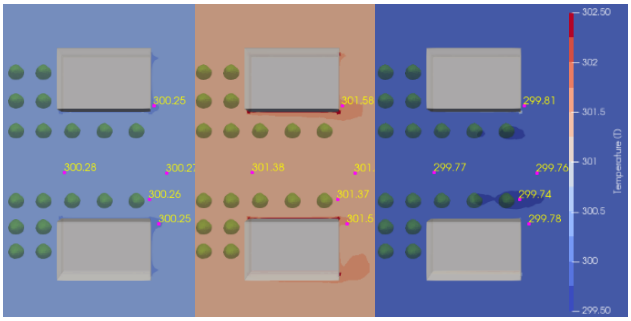

Figure 4.5.1: Air temperature (Left to Right) 11am, 3pm, & 8pm

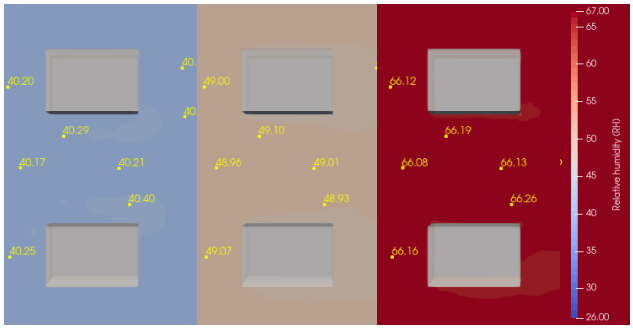

Figure 4.5.2 RH (Left to Right) 11am, 3pm, & 8pm

Graph 4.5.2 showcase the drop in stomatal resistance and increase in Relative humidity (Figure 4.5.2), lowering the air temperatures (Graph 4.5.1 and Figure 4.5.1). This analysis also shows how high seasonal temperatures can adversely affect the smaller tree's cooling potential. A slight reduction in dry bulb temperatures and less stomatal resistance with good LAD values and mid-size or large trees contribute better to the cooling potential of the surroundings

5. Discussion

This study's results and findings highlight vegetation's complex role in regulating urban microclimates. By analyzing detailed iterations, important vegetation parameters, such as tree height, LAD, leaf length, and stomatal resistance, the influence if vegetation on its cooling potential was evaluated through the interrelation of air temperature, Moisture content, leaf temperature, wind velocity, stomatal resistance, and relative humidity.

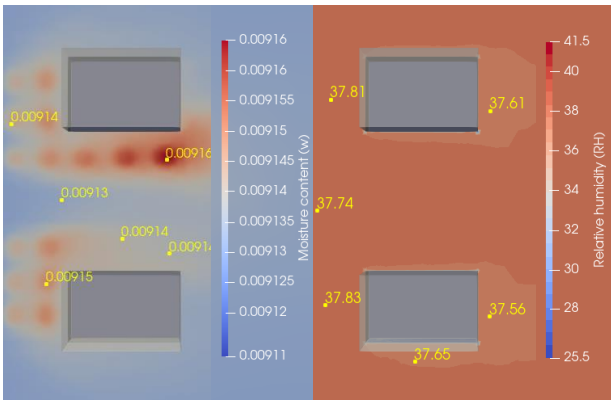

Figure 5.1: Moisture content (left) and RH (right) for Mid-June (3 p.m. to 4 p.m.)

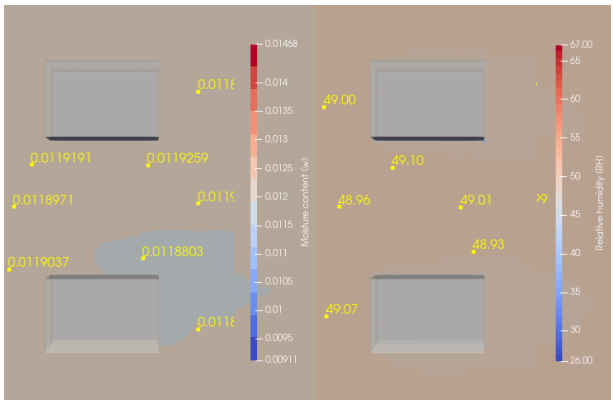

Figure 5.2: Moisture content (left) and RH (right) for Mid-March (3 p.m. to 4 p.m.)

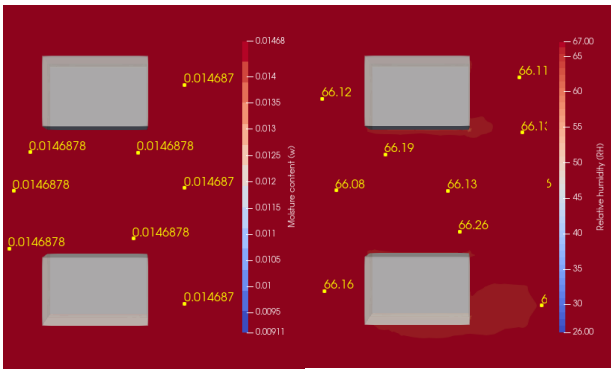

Figure 5.3: Moisture content (left) and RH (right) for Mid-March (7 p.m. to 8 p.m.)

Tree size and LAD appeared to be the most significant parameters affecting urban microclimate. Trees with a height of 7 m or more, along with LAD values of more than 1 m^2/m^3, exhibited reduced air temperature, stabilized moisture content, and relative humidity levels. Due to their larger size, these trees offer more shade and have a higher transpiration rate.

Although Leaf length plays a crucial role in cooling potential the variations of leaf size 0.05m, 0.1m and 0.15m had less impact than LAD values of 0.5 m^2/m^3, 1 m^2/m^3, and 1.5 m^2/m^3.

Figure 5.4 showcases the stomatal resistance variations emphasized the moisture content in the surrounding environment. As the tree size increased, the effect of the stomatal resistance on the moisture content appeared over a larger area. This clearly highlights that the trees or parts of trees undergoing more stomatal resistance showed less moisture content near the respective tree canopy. This spread of the moisture content further resulted in the levels of relative humidity in the air.

The diurnal and seasonal variations demonstrated the sensitivity of vegetation and its cooling potential. Iteration 1 with smaller trees and in June month exacerbated the air temperatures. As per the information by [47], warmer air holds more water vapor, resulting in lower RH than cooler air with the same moisture level. This increase in air was noted along with a reduction in relative humidity without affecting the moisture content of the air. Additionally, [44] the model

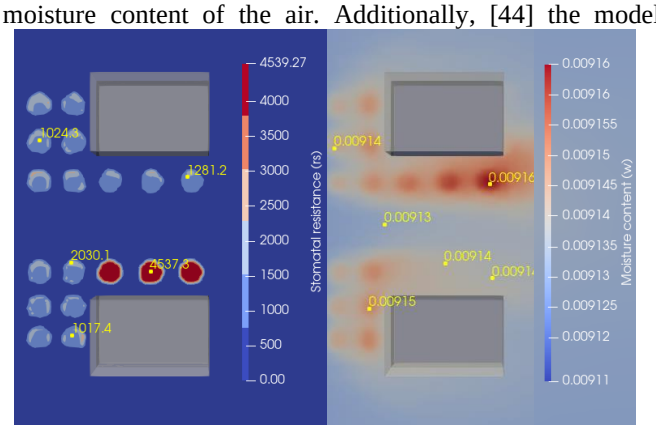

Figure 5.4: Stomatal resistance (left) and Moisture content (right) for Mid-June (3 p.m. to 4 p.m.)

assumes a constant availability of the moisture for root uptake in the soil. This constant source of moisture consideration and stomata being open could also lead to higher moisture calculations.

When we analyzed the results from Iteration 2 (mid-June analysis from 11 a.m. to 4 p.m.) alongside Iteration 2c (mid-March analysis from 11 a.m. to 8 p.m.), we highlighted the reduction in temperature after 4 p.m. in mid-March, along with increase in relative humidity and moisture content (Figures 5.1, 5.2, and 5.3). Iteration 2c, demonstrated that harsh weather conditions can have negatively impact vegetation's cooling potential. One study [24] also highlights how in appropriate combinations of weather, location, and species could adversely affect the UHI mitigation. This finding is extremely crucial considering the year around seasonal changes and it's direct impact on the cooling vegetations cooling abilities.

This study highlights the importance of a comprehensive approach to managing urban microclimates. It suggests that we must consider factors such as tree size, LAD, stomatal resistance, and leaf length and the ease with which water vapour releases through stomata. Achieving the right balance among these elements can enhance cooling and stabilize humidity. Eventually resulting in a more comfortable and sustainable urban microclimate.

Future studies can address the analysis of different species and other urban settings where vegetation and building proportionality ratios can be studied. Additionally, all other months and different climate zones could be studied for a more comprehensive understanding of the vegetation cooling potential.

6. Conclusion

- Larger trees, at least 7 m or higher, with higher LAD values have significant influenced on the cooling potential. They also provide shade and affect larger area with higher moisture content, leading to better RH values and cooling effects.
- While leaf length contributes to the cooling, LAD plays a more significant role in mitigating higher air temperatures.
- Stomatal resistance affects moisture distribution; higher resistance can lead to lower humidity in the nearby areas.
- Study shows that smaller trees, in combination with high air/dry bulb temperature, can increase moisture content but decrease RH, negatively impacting the cooling process.
- Mid-March analysis indicates cooler temperatures at 4 p.m., than mid-June and even lower after 4 p.m. This lowering suggests seasonal as well as more extended duration analysis influence.
- Overall, the study emphasizes the importance of integrating various tree parameters, weather patterns, tree species, and locations to gain a more comprehensive understanding of vegetation's cooling potential.
- It highlights how extreme weather can reduce trees' effectiveness in cooling the urban environment.
- Future research should explore specific tree characteristics, the integration of vegetation, and different urban scenarios to study the vegetation's ability to mitigate the UHI effect.

References

[1] X. Zhou, H. Chen, Impact of urbanization-related land use land cover changes and urban morphology changes on the urban heat island phenomenon, Science of The Total Environment 635 (2018) 1467–1476. https://doi.org/10.1016/j.scitotenv.2018.04.091.

[2] R. Li, Y. Zhao, M. Chang, F. Zeng, Y. Wu, L. (Leon) Wang, J. Niu, X. Shi, N. Gao, Numerical simulation methods of tree effects on microclimate: A review, Renewable and Sustainable Energy Reviews 205 (2024) 114852. https://doi.org/10.1016/j.rser.2024.114852.

[3] A. Kubilay, D. Strebel, D. Derome, J. Carmeliet, Impact of Tree Leaf Area Density on Cooling and Ventilation of an Urban Neighborhood, in: Journal of Physics: Conference Series, IOP Publishing, 2023: p. 9. https://doi.org/10.1088/1742-6596/2654/1/012148.

[4] D.H.S. Duarte, P. Shinzato, C. dos S. Gusson, C.A. Alves, The impact of vegetation on urban microclimate to counterbalance built density in a subtropical changing climate, Urban Climate 14 (2015) 224–239. https://doi.org/10.1016/j.uclim.2015.09.006.

[5] B. Stone Jr, The City and the Coming Climate: Climate Change in the Places We Live., Cambridge: Cambridge University Press., 2012. https://repository.gatech.edu/entities/publication/e63fb304-d1a1-43d1-9a8e-2d0cb72b6859.

[6] R. Buccolieri, J.-L. Santiago, E. Rivas, B. Sanchez, Review on urban tree modelling in CFD simulations: Aerodynamic, deposition and thermal effects, Urban Forestry & Urban Greening 31 (2018) 212–220. https://doi.org/10.1016/j.ufug.2018.03.003.

[7] E. Erell, D. Pearlmutter, T. Willia, Urban Microclimate: Designing the Spaces Between Buildings, Routledge, 2010. https://www.academia.edu/8212936/TITLE_Urban_Microclimate_Designing_the_Spaces_between_Buildings_AUTHORS_Evyatar_Erell_1.

[8] S. Gillner, J. Vogt, A. Tharang, S. Dettmann, A. Roloff, Role of street trees in mitigating effects of heat and drought at highly sealed urban sites, Landscape and Urban Planning 143 (2015) 33–42. https://doi.org/10.1016/j.landurbplan.2015.06.005.

[9] R. Li, F. Zeng, Y. Zhao, Y. Wu, J. Niu, L. (Leon) Wang, N. Gao, X. Shi, CFD simulations of the tree effect on the outdoor microclimate by coupling the canopy energy balance model, Building and Environment 230 (2023) 109995. https://doi.org/10.1016/j.buildenv.2023.109995.

[10] L. Manickathan, T. Defraeye, J. Allegrini, D. Derome, J. Carmeliet, Parametric study of the influence of environmental factors and tree properties on the transpirative cooling effect of trees, Agricultural and Forest Meteorology 248 (2018) 259–274. https://doi.org/10.1016/j.agrformet.2017.10.014.

[11] S. Ponte, N.F. Sonti, T.H. Phillips, M.A. Pavao-Zuckerman, Transpiration rates of red maple (Acer rubrum L.) differ between management contexts in urban forests of Maryland, USA, Sci Rep 11 (2021) 22538. https://doi.org/10.1038/s41598-021-01804-3.

[12] C.R. McDermot, R. Minocha, V.D. Iii, S. Long, T.L.E. Trammell, Red maple (Acer rubrum L.) trees demonstrate acclimation to urban conditions in deciduous forests embedded in cities, PLOS ONE 15 (2020) e0236313. https://doi.org/10.1371/journal.pone.0236313.

[13] A. Aflaki, M. Mirnezhad, A. Ghaffarianhoseini, A. Ghaffarianhoseini, H. Omrany, Z.-H. Wang, H. Akbari, Urban heat island mitigation strategies: A state-of-the-art review on Kuala Lumpur, Singapore and Hong Kong, Cities 62 (2017) 131–145. https://doi.org/10.1016/j.cities.2016.09.003.

[14] A. Hsu, G. Sheriff, T. Chakraborty, D. Manya, Disproportionate exposure to urban heat island intensity across major US cities, Nat Commun 12 (2021) 2721. https://doi.org/10.1038/s41467-021-22799-5.

[15] M. Santamouris, C. Cartalis, A. Synnefa, D. Kolokotsa, On the impact of urban heat island and global warming on the power demand and electricity consumption of buildings—A review, Energy and Buildings 98 (2015) 119–124. https://doi.org/10.1016/j.enbuild.2014.09.052.

[16] M. Santamouris, Energy and Climate in the Urban Built Environment, 1st ed., Routledge, London, 2001. https://doi.org/10.4324/9781315073774.

[17] N.H. Wong, C.L. Tan, D.D. Kolokotsa, H. Takebayashi, Greenery as a mitigation and adaptation strategy to urban heat, Nat Rev Earth Environ 2 (2021) 166–181. https://doi.org/10.1038/s43017-020-00129-5.

[18] A. Tamaskani Esfehankalateh, J. Ngarambe, G.Y. Yun, Influence of Tree Canopy Coverage and Leaf Area Density on Urban Heat Island Mitigation, Sustainability 13 (2021) 7496. https://doi.org/10.3390/su13137496.

[19] C. Yan, Q. Guo, H. Li, L. Li, G.Y. Qiu, Quantifying the cooling effect of urban vegetation by mobile traverse method: A local-scale urban heat island study in a subtropical megacity, Building and Environment 169 (2020) 106541. https://doi.org/10.1016/j.buildenv.2019.106541.

[20] Z. Yu, S. Xu, Y. Zhang, G. Jørgensen, H. Vejre, Strong contributions of local background climate to the cooling effect of urban green vegetation, Sci Rep 8 (2018) 6798. https://doi.org/10.1038/s41598-018-25296-w.

[21] S. Chatterjee, A. Khan, A. Dinda, S. Mithun, R. Khatun, H. Akbari, H. Kusaka, C. Mitra, S.S. Bhatti, Q.V. Doan, Y. Wang, Simulating micro-scale thermal interactions in different building environments for mitigating urban heat islands, Science of The Total Environment 663 (2019) 610–631. https://doi.org/10.1016/j.scitotenv.2019.01.299.

[22] K.R. Gunawardena, M.J. Wells, T. Kershaw, Utilising green and bluespace to mitigate urban heat island intensity, Science of The Total Environment 584–585 (2017) 1040–1055. https://doi.org/10.1016/j.scitotenv.2017.01.158.

[23] J. von Oppen, J.J. Assmann, A.D. Bjorkman, U.A. Treier, B. Elberling, J. Nabe-Nielsen, S. Normand, Cross-scale regulation of seasonal microclimate by vegetation and snow in the Arctic tundra, Glob Chang Biol 28 (2022) 7296–7312. https://doi.org/10.1111/gcb.16426.

[24] H. Li, Y. Zhao, C. Wang, D. Ürge-Vorsatz, J. Carmeliet, R. Bardhan, Cooling efficacy of trees across cities is determined by background climate, urban morphology, and tree trait, Commun Earth Environ 5 (2024) 1–14. https://doi.org/10.1038/s43247-024-01908-4.

[25] J. Chen, S.C. Saunders, T.R. Crow, R.J. Naiman, K.D. Brosofske, G.D. Mroz, B.L. Brookshire, J.F. Franklin, Microclimate in Forest Ecosystem and Landscape Ecology:

Variations in local climate can be used to monitor and compare the effects of different management regimes, BioScience 49 (1999) 288–297. https://doi.org/10.2307/1313612.
[26] X. Feng, H. Wen, M. He, Y. Xiao, Microclimate effects and influential mechanisms of four urban tree species underneath the canopy in hot and humid areas, Front. Environ. Sci. 11 (2023). https://doi.org/10.3389/fenvs.2023.1108002.
[27] R. Richter, H. Ballasus, R.A. Engelmann, C. Zielhofer, A. Sanaei, C. Wirth, Tree species matter for forest microclimate regulation during the drought year 2018: disentangling environmental drivers and biotic drivers, Sci Rep 12 (2022) 17559. https://doi.org/10.1038/s41598-022-22582-6.
[28] A.-S. Yang, Y.-H. Juan, C.-Y. Wen, C.-J. Chang, Numerical simulation of cooling effect of vegetation enhancement in a subtropical urban park, Applied Energy 192 (2017) 178–200. https://doi.org/10.1016/j.apenergy.2017.01.079.
[29] N. Meili, J.A. Acero, N. Peleg, G. Manoli, P. Burlando, S. Fatichi, Vegetation cover and plant-trait effects on outdoor thermal comfort in a tropical city, Building and Environment 195 (2021) 107733. https://doi.org/10.1016/j.buildenv.2021.107733.
[30] A. Hami, B. Abdi, D. Zarehaghi, S.B. Maulan, Assessing the thermal comfort effects of green spaces: A systematic review of methods, parameters, and plants' attributes, Sustainable Cities and Society 49 (2019) 101634. https://doi.org/10.1016/j.scs.2019.101634.
[31] J. Yan, W. Zhou, G.D. Jenerette, Testing an energy exchange and microclimate cooling hypothesis for the effect of vegetation configuration on urban heat, Agricultural and Forest Meteorology 279 (2019) 107666. https://doi.org/10.1016/j.agrformet.2019.107666.
[32] A. Dimoudi, M. Nikolopoulou, Vegetation in the urban environment: microclimatic analysis and benefits, Energy and Buildings 35 (2003) 69–76. https://doi.org/10.1016/S0378-7788(02)00081-6.
[33] Y. Toparlar, B. Blocken, B. Maiheu, G.J.F. van Heijst, A review on the CFD analysis of urban microclimate, Renewable and Sustainable Energy Reviews 80 (2017) 1613–1640. https://doi.org/10.1016/j.rser.2017.05.248.
[34] N. Antoniou, H. Montazeri, M. Neophytou, B. Blocken, CFD simulation of urban microclimate: Validation using high-resolution field measurements, Sci Total Environ 695 (2019) 133743. https://doi.org/10.1016/j.scitotenv.2019.133743.
[35] P. Vanky, Numerical Simulations of the Urban Microclimate, in: 2023. https://www.semanticscholar.org/paper/Numerical-Simulations-of-the-Urban-Microclimate-Vanky/03eaefb43621fe9ac1886de58377d34256c83831 (accessed December 7, 2024).
[36] L. Manickathan, A. Kubilay, T. Defraeye, J. Allegrini, D. Derome, J. Carmeliet, Integrated vegetation model for studying the cooling potential of trees in urban street canyons, in: Healthy, Intelligent and Resilient Buildings and Urban Environments, International Association of Building Physics (IABP), 2018: pp. 547–552. https://doi.org/10.14305/ibpc.2018.gb-2.03.
[37] H. Hiraoka, An investigation of the effect of environmental factors on the budgets of heat, water vapor, and carbon dioxide within a tree, Energy 30 (2005) 281–298. https://doi.org/10.1016/j.energy.2004.05.015.
[38] L. Liang, L. Xiaofeng, L. Borong, Z. Yingxin, Improved k–ε two-equation turbulence model for canopy flow, Atmospheric Environment 40 (2006) 762–770. https://doi.org/10.1016/j.atmosenv.2005.10.010.
[39] H. Majdoubi, T. Boulard, H. Fatnassi, L. Bouirden, Airflow and microclimate patterns in a one-hectare Canary type greenhouse: An experimental and CFD assisted study, Agricultural and Forest Meteorology 149 (2009) 1050–1062. https://doi.org/10.1016/j.agrformet.2009.01.002.
[40] M. Bruse, H. Fleer, Simulating surface–plant–air interactions inside urban environments with a three dimensional numerical model, Environmental Modelling & Software 13 (1998) 373–384. https://doi.org/10.1016/S1364-8152(98)00042-5.
[41] C. Gromke, B. Blocken, W. Janssen, B. Merema, T. van Hooff, H. Timmermans, CFD analysis of transpirational cooling by vegetation: Case study for specific meteorological conditions during a heat wave in Arnhem, Netherlands, Building and Environment 83 (2015) 11–26. https://doi.org/10.1016/j.buildenv.2014.04.022.
[42] M. Robitu, M. Musy, C. Inard, D. Groleau, Modeling the influence of vegetation and water pond on urban microclimate, Solar Energy 80 (2006) 435–447. https://doi.org/10.1016/j.solener.2005.06.015.
[43] Y. Abu-Zidan, P. Mendis, T. Gunawardena, Optimising the computational domain size in CFD simulations of tall buildings, Heliyon 7 (2021). https://doi.org/10.1016/j.heliyon.2021.e06723.
[44] M.O. Mughal, A. Kubilay, S. Fatichi, N. Meili, J. Carmeliet, P. Edwards, P. Burlando, Detailed investigation of vegetation effects on microclimate by means of computational fluid dynamics (CFD) in a tropical urban environment, Urban Climate 39 (2021) 100939. https://doi.org/10.1016/j.uclim.2021.100939.
[45] H. Janssen, B. Blocken, J. Carmeliet, Conservative modelling of the moisture and heat transfer in building components under atmospheric excitation, International Journal of Heat and Mass Transfer 50 (2007) 1128–1140. https://doi.org/10.1016/j.ijheatmasstransfer.2006.06.048.
[46] D. Derome, A. Kubilay, D. Strebel, A. Rubin, J. Carmeliet, Simulation of the local urban climate and its mitigation during heat waves, in: 2021. https://doi.org/10.26868/25222708.2021.31124.
[47] N. US Department of Commerce, Discussion on Humidity, (n.d.). https://www.weather.gov/lmk/humidity (accessed December 11, 2024).